

Electrolytic Conversion of Bicarbonate into CO in a Flow Cell

Tengfei Li,^{1‡} Eric W. Lees,^{2‡} Maxwell Goldman,¹

Danielle A. Salvatore,² David M. Weekes,³ Curtis P. Berlinguette^{1,2,3*}

¹Department of Chemistry, The University of British Columbia, 2036 Main Mall,
Vancouver, BC V6T 1Z1, Canada

²Department of Chemical & Biological Engineering, The University of British
Columbia, 2360 East Mall, Vancouver, BC V6T 1Z3, Canada

³Stewart Blusson Quantum Matter Institute, The University of British Columbia,
2355 East Mall, Vancouver, BC V6T 1Z4, Canada

Correspondence: cberling@chem.ubc.ca

[‡] T.L. and E.W.L. contributed equally

Summary

Electrochemical CO₂ reduction offers a method to use renewable electricity to convert CO₂ into CO and other carbon-based chemical building blocks. While nearly all studies rely on a CO₂ feed, we show herein that aqueous HCO₃⁻ solutions can also be electrochemically converted into CO gas at meaningful rates in a flow cell. We achieved this result in a flow cell containing a bipolar membrane (BPM) and a silver nanoparticle catalyst on a porous carbon support. Electrolysis upon a N₂-saturated 3.0-M KHCO₃ electrolyte solution yields CO with a faradaic efficiency (F.E._{CO}) of 81% at 25 mA cm⁻² and 37% at 100 mA cm⁻². This output is comparable to the analogous experiment where the electrolyte is saturated with gaseous CO₂ (faradaic efficiency for CO is 78% at 25 mA cm⁻² and 35% at 100 mA cm⁻²). The H⁺ flux from the BPM is critical to this chemistry in that it reacts with the HCO₃⁻ feed to generate CO₂, which is then reduced to CO at the gas diffusion electrode. These results are important in that they show that the addition of gaseous CO₂ to HCO₃⁻ electrolytes is not necessary in order to obtain reduced carbon products with a flow cell architecture. This process offers a means of using electrolysis to bypass the thermally-intensive step of extracting CO₂ from HCO₃⁻ solutions generated in carbon capture schemes.

Keywords

electrolysis; flow cell; bicarbonate; carbon dioxide; carbon monoxide; carbon capture and utilization

Introduction

A number of different cell configurations have been proposed in an effort to reach the high current densities and product selectivities that would be required by a commercial CO₂ electrolyzer, yet there is no low-temperature CO₂ electrolyzer available to the market.¹⁻⁷ The majority of cell configurations supply CO₂ to the cathode of the electrochemical cell as a saturated solution in a supporting aqueous electrolyte.^{1,2,7} There are also many examples where gaseous CO₂ is delivered directly to the electrode without a liquid medium.⁸⁻¹² A challenge with CO₂-fed liquid systems is that bubbling gaseous CO₂ into the electrolyte reaches a saturated [CO₂] of ~0.033 M at ambient temperature and pressure prior to and during electrolysis. This saturation point fundamentally limits the maximum current density that can be achieved for CO₂ reduction in the bulk liquid phase.¹³ Furthermore, the addition of CO₂ to the electrolyte causes a lowering in pH resulting in conditions that favour the competing hydrogen evolution reaction (HER) instead of the CO₂ reduction reaction (CO₂RR).¹⁴⁻¹⁶ These characteristics of CO₂-saturated electrolyte systems provide the impetus to explore alternative pathways for accessing electrolytically-reduced carbon products at high current densities.

A system capable of efficiently utilizing bicarbonate (HCO₃⁻) as a source of carbon to form electrochemical products is compelling because the maximum carbon concentration in a saturated aqueous solution of KHCO₃ (~3.3 M) is greater than for saturated CO₂ (33 mM). The ability to convert HCO₃⁻ in solution to a reduced carbon product would also provide an opportunity to avoid electrolyte acidification caused by the addition of gaseous CO₂. However, very few examples of systems capable of these electrochemical transformations currently exist. A study by Hori in 1983 showed that formate could be produced from the electrochemical reduction of a 1.0-M NaHCO₃ solution without a CO₂ supply in an H-cell architecture containing a mercury catalyst, but with a partial current density for formate (J_{formate}) of <1 mA cm⁻².¹⁷ Kanan and coworkers reported in 2015 that a palladium catalyst in an H-cell was able to reduce 2.8-M KHCO₃ into formate without a CO₂ feed at $J_{\text{formate}} = 3.2 \text{ mA cm}^{-2}$ (*c.f.* 6.1 mA cm⁻² in a CO₂-fed HCO₃⁻ solution). To our knowledge, these results set the benchmark for electrochemical HCO₃⁻ conversion to a reduced carbon product in a system without supply of CO₂.¹⁴ All other reports of HCO₃⁻ reduction

chemistry show lower current densities and faradaic efficiencies compared to CO₂-fed systems. Moreover, formate is the only product that has been reported from the reduction of HCO₃⁻ without a CO₂ feed, thus the electrochemical reduction of HCO₃⁻ into CO without a CO₂ supply is not currently known.

Our program has an interest in developing flow cells that mediate CO₂RR at high current densities.¹⁰ Our previous studies have shown that a membrane reactor architecture with a BPM separating the cathode and the anode gas diffusion layers is effective at mediating CO₂RR with CO₂ delivered either as a gas⁸ or as dissolved in aqueous electrolyte.⁹ While a gaseous CO₂ feed enables higher current densities,^{10,18,19} there are practical advantages to delivering liquid rather than gas to the reactor.¹⁰ However, realizing high current densities with a liquid feed is challenging because of the low solubility limits of CO₂. Recognizing that the BPM delivers H⁺ to the cathode, we became intrigued by the possibility that the high H⁺ flux at the BPM could react with HCO₃⁻ to form a high local concentration of CO₂ that would be available for electrochemical reduction at the catalyst,^{20,21} and without the need for an external supply of CO₂.

Following this line of inquiry, we built an electrochemical flow reactor^{8,9} to electrochemically reduce KHCO₃ solutions without the need to supply the electrolyte with gaseous CO₂. We demonstrate herein a 3.0-M KHCO₃ electrolyte yields a F.E._{CO} of 81% at 25 mA cm⁻² that is comparable with a system wherein the electrolyte is saturated with CO₂ gas (F.E._{CO} = 78%). This experiment provides the following unique observations: (i) a carbon product other than formate as the product of electrochemical reduction performed upon a HCO₃⁻ solution; (ii) comparable electrolytic activity measured for HCO₃⁻ electrolytes with and without saturation from a gaseous CO₂ feed; (iii) the electrochemical conversion of HCO₃⁻ solutions in a continuous flow reactor; and (iv) that the BPM in flow cell enhances the conversion of HCO₃⁻ to CO through a CO₂ mediated pathway. These results illuminate an alternative way to electrolytically form carbon-based products derived from CO₂. This methodology also presents a new opportunity for air capture schemes because electrolysis could potentially bypass the energy-intensive thermal extraction of CO₂ gas from HCO₃⁻ solutions.²²

Results and discussion

A two-electrode liquid flow-cell electrochemical reactor was used for our electrochemistry experiments (Figure 1).⁸ The flow cell was built in-house and consists of housing, gaskets, anode and cathode flow-field plates and a membrane electrode assembly (MEA). The anode and cathode housings are made from stainless steel and serve to deliver liquid electrolyte to the anode and cathode. The titanium cathode flow plate and stainless steel anode flow plate sandwich the 4-cm² MEA. The anode (316 stainless steel) and cathode (grade 2 titanium) flow-field plates (active areas = 4 cm²) contain serpentine channels 1.5 mm wide and 1.5 mm deep with 1-mm ribs. The MEA consists of a nickel foam anode (2.5 × 2.5 cm²), a BPM (3 × 3 cm²), and a silver nanoparticle-coated porous carbon support as the cathode (2.5 × 2.5 cm²). The entire assembly is sandwiched between the two stainless housings fastened with 8 bolts. The silver-coated carbon cloth cathode was prepared by spray coating carbon cloth (CeTech) with a mixture of commercially-available silver nanopowder and NafionTM solution. The anode feed was 1.0-M KOH delivered at 50 mL min⁻¹ and the cathode feed was an aqueous solution of either 3.0-M K₂CO₃ or 3.0-M KHCO₃ delivered at 50 mL min⁻¹ continuously purged through the head space with either N₂ or sparged with CO₂ gas at a rate of 160 sccm. Cyclic voltammetry measurements of the two-electrode flow cell were collected over the -1.5 to -3.5 V range (reported as the cell potential). Faradaic efficiencies for CO production were measured at constant cathodic current densities of 25, 50, 75 and 100 mA cm⁻². pH measurements were obtained by diverting ~10 mL of catholyte flowing through the peristaltic pump into a glass vial from which the pH was measured. Gas chromatography (GC) analysis of the gaseous headspace at the electrolyzer outlet showed CO, CO₂, and H₂ as the only detectable products. The cathode solution was analyzed by ¹H NMR after electrolysis and no liquid products were detected. F.E. for CO is reported with the remainder of the electrochemical products confirmed as H₂. Further description of the setup and full cell dimensions are included in the Supplementary Information (Figure S1). Control experiments were also applied using an analogous flow cell architecture with an anion exchange membrane (AEM) in place of the BPM.

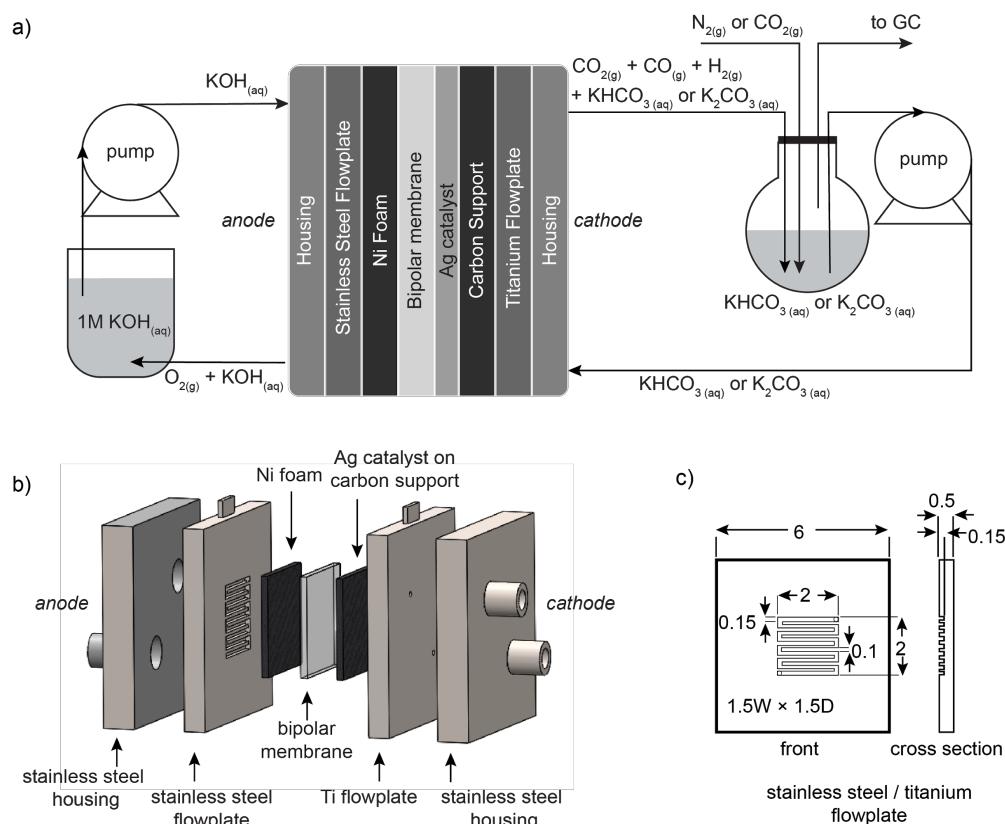


Figure 1. Experimental setup of (a) electrochemical flow cell experiment (b) an expanded view of the flow cell, and (c) dimensions of the cathode & anode flowplates. Nickel foam (anode) and silver deposited on a porous carbon support (cathode) were separated by a BPM. 1.0-M KOH electrolyte was circulated through the stainless flow plate and oxidized into O₂ gas at the anode. Either KHCO₃ or K₂CO₃ electrolyte solutions with CO₂ sparged in or with N₂ purged through the headspace were circulated through the titanium flow plate and reduced into CO at the cathode. The cathodic products were analyzed by gas chromatography (GC). Electrolyte flows were driven by peristaltic pumps at 50 mL min⁻¹. Gas flows (N₂ or CO₂) were set at 160 sccm. All dimension in (d) are in cm.

Electrolysis of HCO₃⁻ solutions produce CO

The flow cell setup described above was used to test the electrochemical production of CO during electrolysis of two 3.0-M KHCO₃ solution systems: (i) KHCO₃ reservoir sparged with CO₂; and (ii) N₂

purged through the headspaces of the KHCO_3 reservoirs. Cyclic voltammograms (CVs) were collected between potentials of -1.0 and -3.5 V (Figure 2a) in a two-electrode flow cell, and F.E._{CO} values were measured between current densities of 25 and 100 mA cm^{-2} in 25- mA cm^{-2} increments (Figure 2b). The viability of the flow cell towards CO_2 reduction was confirmed by results from the CO_2 -saturated 3.0-M KHCO_3 solution (Figure 2, black): The CV exhibits a sharp rise in current density at -2.5 V and a current density of 90 mA cm^{-2} at -3.5 V was measured. The moderate F.E._{CO} of 78% exhibited at low current densities (25 mA cm^{-2}) is further reduced at higher current densities (e.g., 35% at 100 mA cm^{-2}). These results are consistent with previous reports of CO_2 -to-CO reduction in liquid-fed flow cells.^{9,23,24}

Having validated the CO_2RR activity of our flow cell, we then investigated the electrochemical reduction of HCO_3^- in the absence of a CO_2 supply. CVs collected over the -1.0 to -3.5 V cell potential range show similar reductive sweep profiles to the CO_2 -saturated solution (Figure 2a). Peak current density of 100 mA cm^{-2} was measured for the KHCO_3 solution in the absence of CO_2 supply. Electrochemical reduction of N_2 -saturated 3.0-M KHCO_3 solution showed a F.E._{CO} of 81% at a current density of 25 mA cm^{-2} , and 37% at 100 mA cm^{-2} (Figure 2b, orange). These results represent the first observations of the production of CO from a HCO_3^- solution in the absence of a gaseous CO_2 feed, and the first example of producing a reduced carbon product other than formate from HCO_3^- . We note that the difference in F.E._{CO} for the N_2 -saturated 3.0-M KHCO_3 solution with the analogous CO_2 -saturated solution is <2% at every current density between 25 and 100 mA cm^{-2} . Electrochemical reduction of the N_2 -saturated 3.0-M K_2CO_3 solution was also performed following similar procedures and showed a F.E._{CO} of 4.0% at 20 mA cm^{-2} , and 1.0% at 100 mA cm^{-2} (Figure S2). The relatively low F.E._{CO} for the CO_3^{2-} solution confirms that CO_3^{2-} is not electrochemically active.

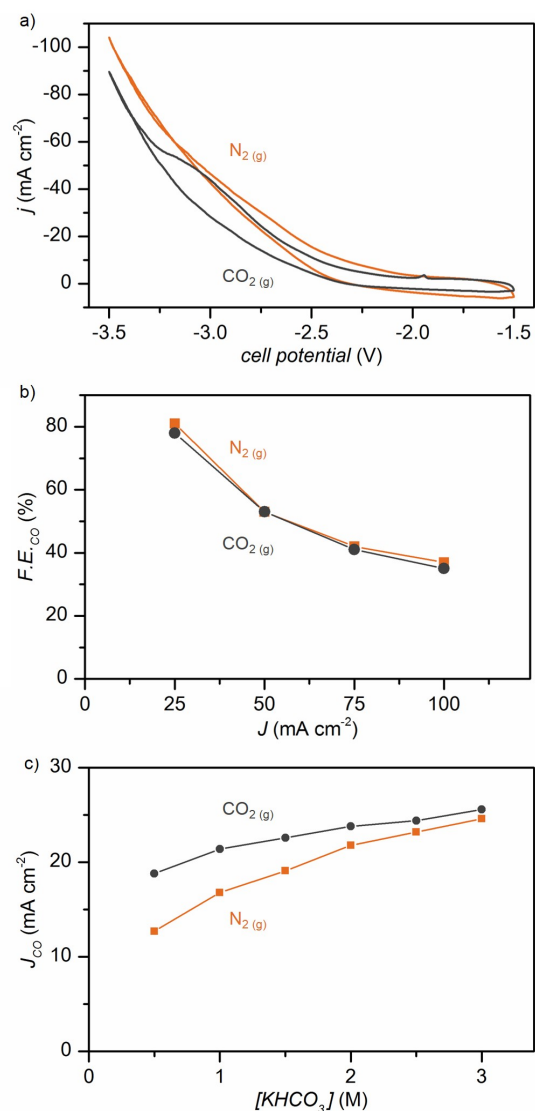


Figure 2. Electrochemical reduction of KHCO_3 solutions sparged with $\text{CO}_2(\text{g})$ (black) and $\text{N}_2(\text{g})$ (orange) in an electrolyzer flow cell containing a BPM show nearly identical behavior: (a) CVs recorded over the -1.5 and -3.5 V range at a scan rate of 100 mV s^{-1} in a 3.0-M KHCO_3 solution; (b) F.E._{CO} measured at constant current densities between 25 and 100 mA cm^{-2} in a 3.0-M KHCO_3 solution; (c) J_{CO} as a function of $[\text{KHCO}_3]$. Cathode: silver deposited on porous carbon support; anode: nickel foam; catholyte: KHCO_3 ; anolyte: 1.0-M KOH. J_{CO} values were measured at a constant cell potential at 3.0 V in a series of KHCO_3 solutions prepared with different HCO_3^- concentrations saturated with CO_2 or N_2 .

The dependence of F.E._{CO} on [HCO₃⁻] was investigated by measuring the partial current densities for CO (J_{CO}) at a constant cell potential of 3.0 V for a series of N₂-saturated and CO₂-saturated KHCO₃ solutions prepared with HCO₃⁻ concentrations ranging from 0.5 M to 3.0 M (Figure 2c). The results show that increasing [KHCO₃] increases the J_{CO} from 13 mA cm⁻² at 0.5 M to 25 mA cm⁻² at 3.0 M. The same solutions bubbled with CO₂ show a similar (but less pronounced) increase in J_{CO} from 19 mA cm⁻² at 0.5-M KHCO₃ to 26 mA cm⁻² at 3.0-M KHCO₃. The F.E._{CO} and total current densities for each electrolyte are provided in Figure S3. The J_{CO} for solutions with <2 M of KHCO₃ (where most CO₂RR studies are performed) were significantly greater in each case for the CO₂-fed electrolytes. The N₂-saturated solution yields J_{CO} values comparable with those measured for the CO₂-saturated solution at [KHCO₃] > 2.5 M. An increase in J_{CO} values with increasing [HCO₃⁻] (for both the N₂-saturated and the CO₂-saturated solutions) is consistent with HCO₃⁻ enhancing the rate of the electrochemical reduction of CO₂ through a rapid exchange with CO₂^{25,26} or suppression of HER with increasing electrolyte pH.¹⁴

Defining the reactions in the flow cell

Resolving the electrochemically active species in the flow reactor is made challenging by the closed reaction vessel and the dynamic acid-base equilibria that defines the relative concentrations of CO₂, HCO₃⁻, and CO₃²⁻. We therefore designed a set of experiments to confirm that the amount of CO produced from a HCO₃⁻ stream is governed by three key processes: (i) an acid/base equilibrium of HCO₃⁻ with protons supplied by the BPM to form CO₂ and H₂O at the membrane-solution interface; (ii) the reduction of this *in-situ* generated CO₂ to CO and OH⁻; and (iii) the *in-situ* generated OH⁻ increasing the bulk pH to favor CO₃²⁻ formation, which inhibits CO production (Figure 3a). We operated a flow cell with either a BPM or an AEM at 100 mA cm⁻² for 2 hours and measured F.E._{CO} while tracking the concentration of CO_{2(g)} leaving the flow cell ([CO₂]_{outlet}) and the pH of the bulk catholyte solutions (Figure 3a). We also operated the flow cell containing the BPM, but while circulating KHCO₃ without an applied potential (denoted BPM/no electrolysis). These experiments showed that the [CO₂]_{outlet} decreased over time with both the BPM and

AEM, and that the $[\text{CO}_2]_{\text{outlet}}$ measured with the BPM system is higher than that measured for the AEM and BPM/no electrolysis (Figure 4a). The formation of CO_2 on the cathodic side of the BPM membrane was confirmed by an independent experiment with an H-cell, where operation at 20 mA cm^{-2} produced enough CO_2 to exceed the solubility limit of CO_2 (Figure 4d). We also observed a correlation of F.E._{CO} to $[\text{CO}_2]_{\text{outlet}}$ for both the BPM and AEM (Figure 4c), where F.E._{CO} decreases with $[\text{CO}_2]_{\text{outlet}}$ as a function of time. Finally, the pH of the catholyte increased as a function of time for all three experiments (Figure 4b), where electrolysis accelerated the change in alkalinity.

These collective experimental results support the cathodic reaction chemistry listed in Figure 3b. The higher $[\text{CO}_2]_{\text{outlet}}$ measured with the BPM than with the AEM is consistent with the BPM supplying a flux of H^+ that is available for reaction with HCO_3^- to form CO_2 (Figure 3b). This conclusion is further supported by the higher $[\text{CO}_2]_{\text{outlet}}$ measured when the flow cell with the BPM is subjected to electrolysis (and thus creating a higher $[\text{H}^+]$ at the cathode) relative to the experiment without an applied potential. We interpret the linear relationship that exists between F.E._{CO} and the $[\text{CO}_2]_{\text{outlet}}$ for both membranes as an indication that CO_2 is the electrochemically active species; i.e., a higher amount of CO_2 available enables more CO to be generated through CO_2RR at the catalyst. This correlation is also consistent with the BPM yielding a higher local CO_2 concentration at the catalyst.

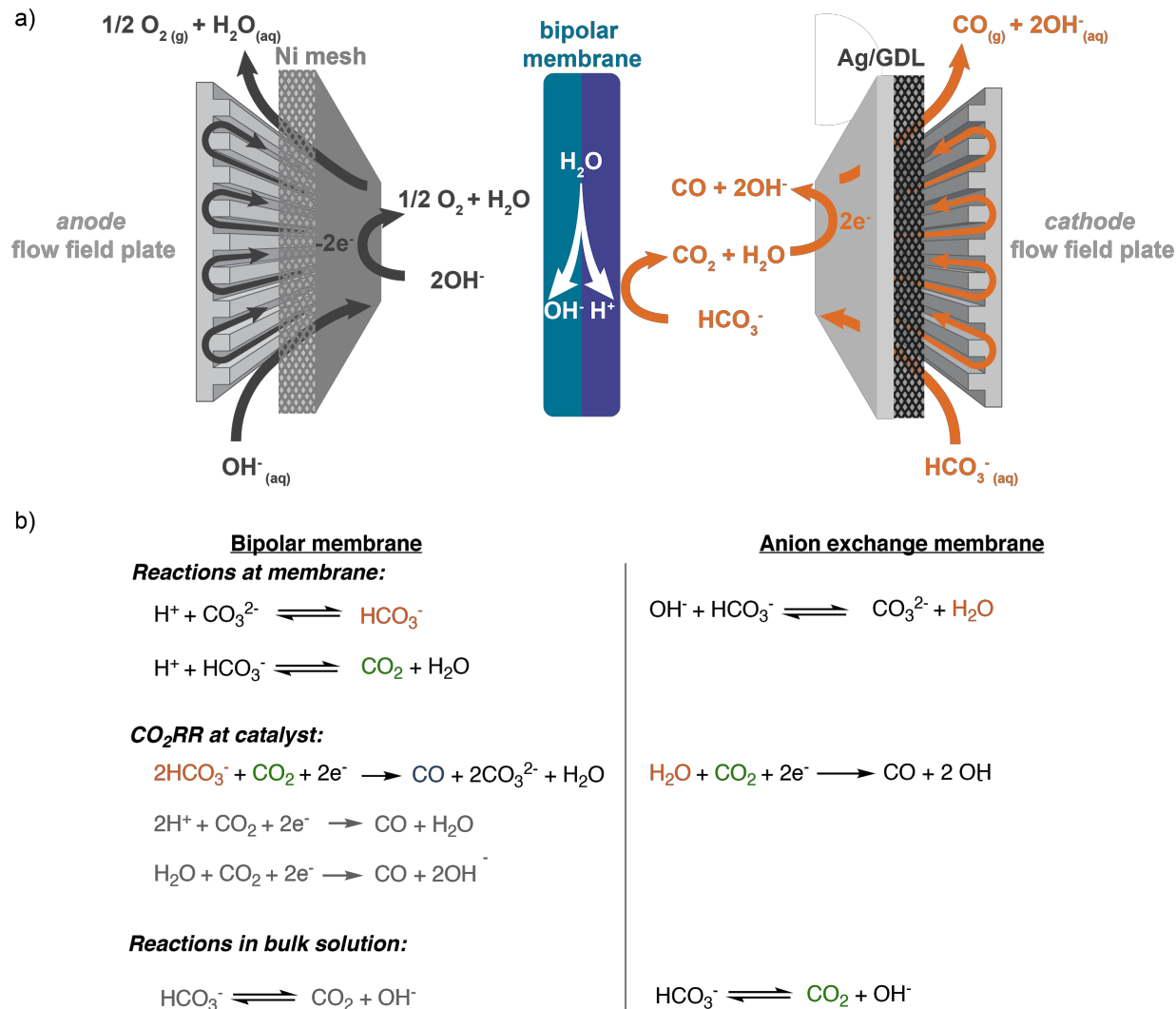


Figure 3. a) Schematic representation of the dominant chemical and electrochemical reactions occurring in the flow cell containing a BPM: Reaction of H^+ with HCO_3^- to form CO_2 at the membrane interface, and the electrochemical reduction of CO_2 at the catalyst to form CO and OH^- . b) Summary of the reaction chemistry at the membrane and catalyst surfaces and in the bulk solutions in the cathode reaction compartment when a BPM and AEM are used. The most reactive H^+ donors (orange) and electrochemically active species (green) that dominate reactivity are highlighted. The reactions indicated in light grey are not expected to govern the reaction chemistry.

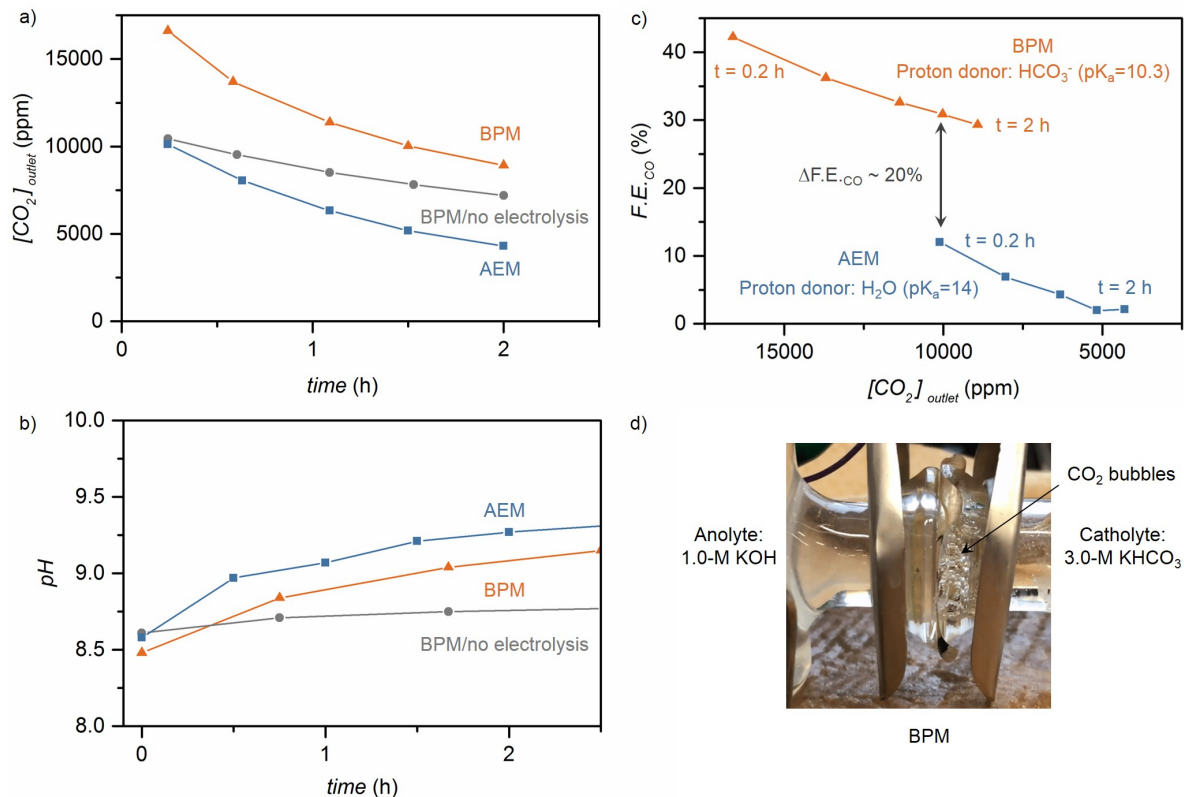


Figure 4. Temporal change in (a) $[CO_2]_{outlet}$ and (b) pH during electrolysis of 3.0 M $KHCO_3$ at 100 mA cm^{-2} with a BPM (orange) or AEM (blue). A control experiment, BPM/no electrolysis (grey), was recorded in a flow cell containing a BPM with the circulation of catholyte without an applied potential. (c) $F.E._{CO}$ as a function of $[CO_2]_{outlet}$ during the 2-h electrolysis of a 3.0-M $KHCO_3$ solution at 100 mA cm^{-2} with a BPM (orange) and an AEM (blue). The $\sim 20\%$ difference in $F.E._{CO}$ values at the same $[CO_2]_{outlet}$ is attributed to the difference in pK_a values of the indicated H^+ donors in the BPM and AEM flow cells. The headspace was purged with a 160 mL/min N_2 stream for all experiments. (d) Image of an H-cell where a BPM separates a silver-coated carbon gas diffusion electrode in the cathodic compartment and a Pt mesh anode in the anodic compartment. The formation of CO_2 bubbles during the electrolysis of HCO_3^- at a current density of 20 mA cm^{-2} confirm enough CO_2 is produced to exceed the solubility limits of CO_2 in aqueous media.

The $\sim 20\%$ higher $F.E._{CO}$ values obtained with the BPM relative to the AEM at the same $[CO_2]_{outlet}$ (e.g., 10,000 ppm) also point to differences in H^+ donors available at the CO_2RR electrocatalyst surfaces.

Considering that the H^+ donors available with the BPM are HCO_3^- , H^+ , and H_2O (Figure 3b), we can assume HCO_3^- to be the most active H^+ donor because the pK_a of 10.3 is lower than that of H_2O ($\text{pK}_a = 14.0$), and the high pH would diminish the role of H^+ . The protons delivered by the BPM would also facilitate the conversion of CO_3^{2-} into HCO_3^- , which could then be converted to CO_2 through acid/base equilibria. In the case where the AEM is used, the build up of OH^- would deplete HCO_3^- near the membrane surface leaving H_2O as the sole H^+ donor for CO_2RR (Figure 3b). On this basis, we conclude that a higher concentration of H^+ donors provided by the BPM than the AEM is responsible for the 20-% difference in F.E._{CO} at a constant $[\text{CO}_2]_{\text{outlet}}$.

Finally, we are able to rationalize the observed increase in pH of the KHCO_3 catholyte solution during electrolysis with both the BPM and AEM systems to be a consequence of OH^- being generated from both HER and CO_2RR at the catalyst (Figure 4c). In accordance with previous models,^{27,28} this increase in pH would decrease F.E._{CO} over the course of our electrolysis experiments where the catholyte solutions are not recycled. The higher F.E._{CO} values could indeed be recovered by replenishing the catholyte with KHCO_3 (Figure S4). An additional advantage over the AEM is that the BPM suppresses the increase of the pH of the catholyte during electrolysis (thereby slowing the shift in the equilibrium of carbon species in solution towards catalytically inactive CO_3^{2-} ; Figures S5-S6) by delivering protons to react with CO_3^{2-} to form HCO_3^- .

This collection of experiments point to the conversion of HCO_3^- to CO being enabled by: (i) an acidic region at the membrane interface; and (ii) a basic region at the catalyst. The acidic membrane interface enables CO_3^{2-} to be converted into HCO_3^- , and HCO_3^- to be converted into catalytically active $\text{CO}_{2(\text{g})}$. The basic pH region at the catalyst layer arises from CO_2RR chemistry that generates OH^- concomitant with CO production. An important outcome of this study is the demonstration that the BPM can deliver a local concentration of CO_2 to the catalyst that exceeds the solubility limits of CO_2 in aqueous media. The ability for the membrane to enable a high concentration of CO_2 at the basic catalyst layer offers a strategy for realizing higher CO_2RR current densities from aqueous feedstocks. This HCO_3^- reduction system also offers the additional advantage of not requiring a CO_2 feed that would acidify the reaction

medium and enable HER.

Conclusions

We demonstrate that HCO_3^- can be reduced to CO in a flow cell containing a BPM without a supply of CO_2 gas to the electrolyte. The observation that a 3.0-M KHCO_3 system without a CO_2 feed yields a comparable faradaic efficiency for CO with a similar system with a CO_2 -fed solution was not expected given that it is widely assumed that a CO_2 feed is necessary for CO production. The BPM plays a critical role in this reaction chemistry by delivering a H^+ flux to the cathode that converts HCO_3^- (and CO_3^{2-}) into catalytically active CO_2 . An important feature of this flow reactor is that the *in-situ* generation of CO_2 provides a higher concentration of CO_2 at the catalyst surface than the solubility limits of CO_2 in aqueous media. This finding offers new opportunities for realizing high current densities with a liquid feed. This work also demonstrates that carbon products other than formate can be generated from HCO_3^- solutions, thereby presenting new opportunities for carbon capture and utilization schemes.

Experimental Procedures

Materials:

KHCO_3 (99%) and K_2CO_3 (99%) were purchased from Alfa Aesar. Ag nanopowder (trace metal basis, 99%) and Nafion 117 solution (5 wt%, in a mixture of lower aliphatic alcohols and water) were purchased from Sigma Aldrich. Carbon cloth was purchased from the Fuel Cell Store and cut into desired dimensions with a blade. Nickel foam gas diffusion electrode material was purchased from MTI. BPM (Fumasep FBM) were purchased from FuMA-tech and stored in 1M NaCl Solution.

Electrode preparation:

The cathode catalyst ink was prepared by mixing 52 mg of silver nanopowder, 500 μL of DI water, 500 μL of isopropyl alcohol and 70 μL Nafion 117 solution. The catalyst ink was then spray-coated on a 4-cm² area of carbon cloth and dried under a gentle air stream. Kapton tape (McMaster-Carr) was used as a mask during the deposition process to avoid catalyst being deposited outside the active area of the carbon cloth. The catalyst loading was determined to be 100-120 counts per second by X-Ray fluorescence analysis.

Electrochemical measurement and product analysis:

A CH instruments 660D with a picoamp booster was used for all experiments. Electrochemical measurements were made with a two-electrode system with Ni foam as the anode and Ag spray-coated on carbon cloth as the cathode. The anode electrolyte was 1000 mL of 1 M KOH solution delivered by a peristaltic pump at 50 mL/min. The cathode electrolyte was 125 mL of 3 M K₂CO₃ or 0.5 ~ 3 M KHCO₃ with 0.02 M ethylenediaminetetraacetic acid (EDTA, 99%, Sigma Aldrich) added to remove impurities.²⁹ The head space of the catholyte solution was purged with N₂ (Praxair, 99.9%) or CO₂ (Praxair, 99.9%) gas at 160 sccm in a sealed flask with an outlet into the flow cell. The catholyte solution was delivered by another peristaltic pump at 50 mL/min into the flow cell electrolyzer, which was then vented back into the flask. Fresh electrolyte was used for each set of experiment. Samples of the gas headspace in the flask were delivered into a gas chromatograph (GC, Perkin Elmer). The GC was equipped with a packed MolSieve 5A column and a packed HayeSepD column. Argon (Praxair, 99.999%) was used as the carrier gas. A flame ionization detector (FID) equipped with a methanizer was used to quantify CO and CO₂ concentrations and a thermal conductivity detector (TCD) was used to quantify H₂ concentrations. Control experiments with a two-compartment H-cell were performed wherein the anode (platinum mesh) and cathode (Ag-coated carbon cloth) compartments contained 30 mL of 1 M KOH and 30 mL of 3.0-M KHCO₃, respectively, separated by a BPM.

Acknowledgements: Funding from The University of British Columbia 4YF Program, Canada Foundation for Innovation, Canada Research Chairs, Quantum Materials and Future Technologies Program, NSERC,

and CIFAR is gratefully acknowledged. Jacky Chau fabricated the gas diffusion electrodes used in this study.

Author contributions: C.P.B. supervised the project. C.P.B., T.L, M.G., E.W.L, D.A.S. designed the experiments. T.L. performed the proof-of-concept study. D.A.S. designed flow cell assembly and experimental setup. E.W.L. and M.G. defined the reactions in the flow cell. All authors contributed to manuscript writing.

Declaration of Interests: The authors declare no competing financial interests.

References:

1. Kuhl, K.P., Cave, E.R., Abram, D.N., and Jaramillo, T.F. (2012). New insights into the electrochemical reduction of carbon dioxide on metallic copper surfaces. *Energy Environ. Sci.* 5, 7050–7059.
2. Qiao, J., Liu, Y., Hong, F., and Zhang, J. (2014). A review of catalysts for the electroreduction of carbon dioxide to produce low-carbon fuels. *Chem. Soc. Rev.* 43, 631–675.
3. Lin, S., Diercks, C.S., Zhang, Y.-B., Kornienko, N., Nichols, E.M., Zhao, Y., Paris, A.R., Kim, D., Yang, P., Yaghi, O.M., *et al.* (2015). Covalent organic frameworks comprising cobalt porphyrins for catalytic CO₂ reduction in water. *Science* 349, 1208–1213.
4. Liu, M., Pang, Y., Zhang, B., De Luna, P., Voznyy, O., Xu, J., Zheng, X., Dinh, C.T., Fan, F., Cao, C., *et al.* (2016). Enhanced electrocatalytic CO₂ reduction via field-induced reagent concentration. *Nature* 537, 382–386.
5. Li, T., Cao, Y., He, J., and Berlinguette, C.P. (2017). Electrolytic CO₂ Reduction in Tandem with

Oxidative Organic Chemistry. ACS Cent. Sci. 3, 778–783.

6. Mariano, R.G., McKelvey, K., White, H.S., and Kanan, M.W. (2017). Selective increase in CO₂ electroreduction activity at grain-boundary surface terminations. *Science* 358, 1187–1192.
7. He, J., Johnson, N.J.J., Huang, A., and Berlinguette, C.P. (2018). Electrocatalytic Alloys for CO₂ Reduction. *ChemSusChem* 11, 48–57.
8. Salvatore, D.A., Weekes, D.M., He, J., Dettelbach, K.E., Li, Y.C., Mallouk, T.E., and Berlinguette, C.P. (2018). Electrolysis of Gaseous CO₂ to CO in a Flow Cell with a Bipolar Membrane. *ACS Energy Lett.* 3, 149–154.
9. Li, Y.C., Zhou, D., Yan, Z., Gonçalves, R.H., Salvatore, D.A., Berlinguette, C.P., and Mallouk, T.E. (2016). Electrolysis of CO₂ to Syngas in Bipolar Membrane-Based Electrochemical Cells. *ACS Energy Lett.* 1, 1149–1153.
10. Weekes, D.M., Salvatore, D.A., Reyes, A., Huang, A., and Berlinguette, C.P. (2018). Electrolytic CO₂ Reduction in a Flow Cell. *Acc. Chem. Res.* 51, 910–918.
11. Whipple, D.T., Finke, E.C., and Kenis, P.J.A. (2010). Microfluidic Reactor for the Electrochemical Reduction of Carbon Dioxide: The Effect of pH. *Electrochem. Solid-State Lett.* 13, B109–B111.
12. Kutz, R.B., Chen, Q., Yang, H., Sajjad, S.D., Liu, Z., and Masel, I.R. (2017). Sustainion Imidazolium-Functionalized Polymers for Carbon Dioxide Electrolysis. *Energy Technol.* 5, 929–936.
13. Weng, L.-C., Bell, A.T., and Weber, A.Z. (2018). Modeling gas-diffusion electrodes for CO₂ reduction. *Phys. Chem. Chem. Phys.* 20, 16973–16984.
14. Min, X., and Kanan, M.W. (2015). Pd-catalyzed electrohydrogenation of carbon dioxide to formate: high mass activity at low overpotential and identification of the deactivation pathway. *J. Am. Chem.*

Soc. *137*, 4701–4708.

15. Zhong, H., Fujii, K., Nakano, Y., and Jin, F. (2015). Effect of CO₂ Bubbling into Aqueous Solutions Used for Electrochemical Reduction of CO₂ for Energy Conversion and Storage. *J. Phys. Chem. C* *119*, 55–61.
16. Kortlever, R., Tan, K.H., Kwon, Y., and Koper, M.T.M. (2013). Electrochemical carbon dioxide and bicarbonate reduction on copper in weakly alkaline media. *J. Solid State Electrochem.* *17*, 1843–1849.
17. Hori, Y., and Suzuki, S. (1983). Electrolytic Reduction of Bicarbonate Ion at a Mercury Electrode. *J. Electrochem. Soc.* *130*, 2387–2390.
18. Dinh, C.-T., Burdyny, T., Kibria, M.G., Seifitokaldani, A., Gabardo, C.M., García de Arquer, F.P., Kiani, A., Edwards, J.P., De Luna, P., Bushuyev, O.S., *et al.* (2018). CO₂ electroreduction to ethylene via hydroxide-mediated copper catalysis at an abrupt interface. *Science* *360*, 783–787.
19. Verma, S., Hamasaki, Y., Kim, C., Huang, W., Lu, S., Jhong, H.-R.M., Gewirth, A.A., Fujigaya, T., Nakashima, N., and Kenis, P.J.A. (2018). Insights into the Low Overpotential Electroreduction of CO₂ to CO on a Supported Gold Catalyst in an Alkaline Flow Electrolyzer. *ACS Energy Lett.* *3*, 193–198.
20. Eisaman, M.D., Parajuly, K., Tuganov, A., Eldershaw, C., Chang, N., and Littau, K.A. (2012). CO₂ extraction from seawater using bipolar membrane electrodialysis. *Energy & Environmental Science* *5*, 7346–7352.
21. Willauer, H.D., Hardy, D.R., Lewis, M.K., Ndubizu, E.C., and Williams, F.W. (2010). Extraction of CO₂ from Seawater and Aqueous Bicarbonate Systems by Ion-Exchange Resin Processes. *Energy Fuels* *24*, 6682–6688.

22. Keith, D.W., Holmes, G., St. Angelo, D., and Heidel, K. (2018). A Process for Capturing CO₂ from the Atmosphere. *Joule* 2, 1573–1594.
23. Dufek, E.J., Lister, T.E., and McIlwain, M.E. (2011). Bench-scale electrochemical system for generation of CO and syn-gas. *J. Appl. Electrochem.* 41, 623–631.
24. Delacourt, C., Ridgway, P.L., Kerr, J.B., and Newman, J. (2008). Design of an Electrochemical Cell Making Syngas (CO + H₂) from CO₂ and H₂O Reduction at Room Temperature. *J. Electrochem. Soc.* 155, B42–B49.
25. Dunwell, M., Lu, Q., Heyes, J.M., Rosen, J., Chen, J.G., Yan, Y., Jiao, F., and Xu, B. (2017). The Central Role of Bicarbonate in the Electrochemical Reduction of Carbon Dioxide on Gold. *J. Am. Chem. Soc.* 139, 3774–3783.
26. Zhu, S., Jiang, B., Cai, W.-B., and Shao, M. (2017). Direct Observation on Reaction Intermediates and the Role of Bicarbonate Anions in CO₂ Electrochemical Reduction Reaction on Cu Surfaces. *J. Am. Chem. Soc.* 139, 15664–15667.
27. Singh, M.R., Kwon, Y., Lum, Y., Ager, J.W., and Bell, A.T. (2016). Hydrolysis of Electrolyte Cations Enhances the Electrochemical Reduction of CO₂ over Ag and Cu. *J. Am. Chem. Soc.* 138, 13006–13012.
28. Gupta, N., Gattrell, M., and MacDougall, B. (2006). Calculation for the cathode surface concentrations in the electrochemical reduction of CO₂ in KHCO₃ solutions. *J. Appl. Electrochem.* 36, 161–172.
29. Wuttig, A., and Surendranath, Y. (2015). Impurity Ion Complexation Enhances Carbon Dioxide Reduction Catalysis. *ACS Catal.* 5, 4479–4484.